

Superconductivity in Ternary Zirconium Telluride Zr_6RuTe_2

Kosuke Yuchi*, Haruka Matsumoto, Daisuke Nishio-Hamane, Kodai Moriyama, Keita Kojima,
Ryutaro Okuma, Jun-ichi Yamaura, and Yoshihiko Okamoto

Institute for Solid State Physics, University of Tokyo, Kashiwa 277-8581, Japan

Zr_6CoAl_2 -type Zr_6RuTe_2 is found to show bulk superconductivity below the superconducting transition temperature $T_c = 1.1$ K, according to the electrical resistivity, magnetization, and heat capacity measurements using synthesized polycrystalline samples. This T_c exceeds that of Zr_6MTe_2 compounds in which M is other transition metals, indicating that M = Ru is favorable for superconductivity in Zr_6CoAl_2 -type Zr_6MX_2 .

Recently, several new superconductors have been discovered in Zr_6CoAl_2 -type A_6MX_2 compounds exhibiting a noncentrosymmetric $P\bar{6}2m$ space group. This finding was initiated by Sc_6MTe_2 , which was reported to exhibit bulk superconductivity for seven transition-metal elements M,¹⁾ followed by several Zr_6MX_2 compounds.²⁻⁴⁾ A unique feature of this superconductor family is M dependence of the superconducting transition temperature, T_c . In Sc_6MTe_2 and Zr_6MTe_2 compounds, the highest T_c is recorded for M = Fe ($T_c = 4.7$ K for Sc_6FeTe_2 and 0.76 K for Zr_6FeTe_2). In contrast, Zr_6MBi_2 superconductors showed a different M dependence of T_c . Zr_6RuBi_2 exhibits a significantly elevated T_c of 4.9 K compared to Zr_6FeBi_2 ($T_c = 1.4$ K). Although the Fe 3d electrons are suggested to contribute to the realization of a high T_c in Sc_6FeTe_2 ,^{1,5)} the highest T_c of Zr_6RuBi_2 among all A_6MX_2 compounds indicates a complex chemical trend in these superconductors, highlighting the importance of continued exploration of new A_6MX_2 superconductors. Recently, superconducting properties other than T_c have also been revealed using microscopic probes such as NMR and μSR .^{6,7)}

In this short note, we focus on Zr_6RuTe_2 , which crystallizes in the hexagonal Zr_6CoAl_2 -type structure.⁸⁾ There have been no previous reports on its electronic properties. We prepared polycrystalline samples of Zr_6RuTe_2 and found that it is a bulk superconductor with $T_c = 1.1$ K.

Polycrystalline samples of Zr_6RuTe_2 were synthesized and characterized using the same procedure as described in Ref. 4. A 6:1:2.1 molar ratio of Zr chips (99.9%, RARE METALLIC), Ru powder (99.95%, RARE METALLIC), and Te powder (99.99%, RARE METALLIC) was arc-melted, and the resulting button was annealed at 1373 K for 216 h. Powder X-ray diffraction (XRD) measurements of Zr_6RuTe_2 polycrystalline samples were conducted at BL02B2 in SPring-8. The X-ray wavelength was $\lambda = 0.354978$ Å. Structural analysis was performed utilizing Rietveld method on JANA2006 software.⁹⁾ The XRD pattern at room temperature is accurately represented by the hexagonal

Zr_6CoAl_2 -type structural model, with lattice parameters $a = 7.8203(3)$ Å and $c = 3.6220(2)$ Å, consistent with the previous study.⁸⁾ The reliability factors of the refinement are $R_{\text{wp}} = 7.92\%$, $R_p = 5.80\%$, and $S = 3.13$. Microstructural observations and chemical analyses were carried out using a scanning electron microscope (SEM; JEOL IT-100) equipped with an attachment for energy-dispersive X-ray spectroscopy (EDX; 15 kV, 0.8 nA, 1 μm beam diameter). The inset of Fig. 1(a) shows that the Zr_6RuTe_2 polycrystalline sample comprises not only the Zr_6RuTe_2 phase (region marked A), representing 89% of the total area, but also the ZrRu and Zr phases (region marked B).¹⁰⁾ The volume fraction of the Zr_6RuTe_2 phase was significantly increased by annealing. The chemical composition of the Zr_6RuTe_2 phase, as determined by EDX, was $\text{Zr}_{6.00(2)}\text{Ru}_{0.93(2)}\text{Te}_{2.07(1)}$. Considering the small degree of nonstoichiometry, the chemical formula of the Zr_6RuTe_2 phase is expressed as Zr_6RuTe_2 in this study. Electrical resistivity and heat capacity were measured using a Physical Property Measurement System (Quantum Design). Magnetization measurements were performed using an MPMS-3 (Quantum Design).

Figures 1(a) and 1(b) display the temperature dependence of the electrical resistivity, ρ , of the Zr_6RuTe_2 polycrystalline sample. As shown in Fig. 1(a), Zr_6RuTe_2 exhibits metallic behavior. The residual resistivity ratio $\text{RRR} = \rho_{300\text{ K}}/\rho_0$ was estimated to be 6.9, where $\rho_{300\text{ K}}$ and ρ_0 denote the ρ at 300 K and the residual resistivity, respectively. As the temperature was further lowered, ρ slightly decreased at $T^* = 1.8$ K and became nearly constant at approximately 1.5 K, as shown in Fig. 1(b). Subsequently, ρ dropped sharply to zero between 1.3 and 1.0 K. This sharp drop was suppressed to lower temperatures under applied magnetic fields, strongly suggesting a superconducting transition. As shown in Fig. 1(c), the zero-field-cooled (ZFC) and field-cooled (FC) magnetization data of the Zr_6RuTe_2 polycrystalline sample under a magnetic field of 10 Oe exhibited a pronounced diamagnetic signal below 1.1 K with a subdued diamagnetic signal below 1.8 K. The shielding fraction at 0.4 K was eval-

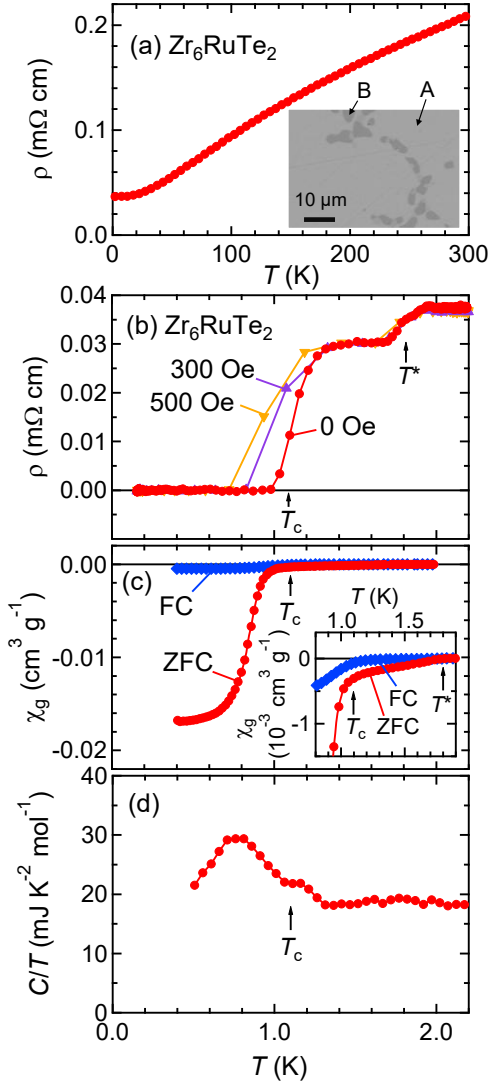


Figure 1. Electronic properties of polycrystalline samples of Zr_6RuTe_2 . (a) Temperature dependence of electrical resistivity above 2 K. The inset shows SEM image of a Zr_6RuTe_2 polycrystalline sample. (b) Temperature dependences of electrical resistivity measured under magnetic fields of 0, 300, and 500 Oe. (c) Temperature dependences of FC and ZFC magnetic susceptibility measured under a magnetic field of 10 Oe. The inset shows an enlarged view of the main panel. (d) Temperature dependence of heat capacity divided by temperature, C/T , measured in zero magnetic field. The C/T values were calculated based on the assumption that the sample consists of a single phase of Zr_6RuTe_2 .

uated to be 165%, assuming the single phase of Zr_6RuTe_2 . The fraction well beyond 100% is probably due to a demagnetization effect.^{11–13} Figure 1(d) shows the heat capacity divided by temperature, C/T , which increases with decreasing temperature below 1.2 K and exhibited a peak at 0.8 K. These results clearly indicate that the Zr_6RuTe_2 polycrystalline samples exhibit bulk superconductivity. Based on the midpoint of the resistivity drop and the onset of the strong magnetization drop below 1.3 K, T_c was

determined to be 1.1 K.

The weak decrease of ρ at T^* is most likely due to the superconductivity of an impurity phase, because a small diamagnetic signal is observed between T^* and T_c in the magnetic susceptibility data and no anomaly appears near T^* in the C/T data. The Zr_6RuTe_2 polycrystalline samples used in this study contained approximately 10% ZrRu and Zr impurity phases. However, these impurity phases do not exhibit superconductivity at T^* . Zr is a known superconductor with $T_c = 0.6$ K.^{14,15} We synthesized a ZrRu polycrystalline sample and found that the ZrRu sample does not exhibit superconductivity above 0.2 K. Therefore, the origin of the weak decrease of ρ at T^* remains as an open question.

The observed $T_c = 1.1$ K of Zr_6RuTe_2 is the highest among Zr_6MTe_2 compounds, although it is lower than the T_c of other Ru-based compounds, such as Zr_6RuBi_2 and Sc_6RuTe_2 .^{1,4} In the Zr_6MTe_2 series, compounds with $\text{M} = \text{Fe}$ and Co exhibit $T_c = 0.76$ K and 0.13 K, respectively, whereas those with $\text{M} = \text{Cr}$ and Mn do not show zero resistivity above 0.1 K.² The M dependence of T_c of Zr_6MTe_2 is similar to that of Zr_6MBi_2 , where Zr_6RuBi_2 has a significantly elevated T_c compared to Zr_6FeBi_2 .⁴ This M dependence differs from that of Sc_6MTe_2 . Sc_6FeTe_2 exhibits the highest T_c among the eight Sc_6MTe_2 compounds synthesized thus far. In Sc_6FeTe_2 , both the Sc 3d and Fe 3d electrons have a large contribution to the density of states at the Fermi energy E_F , which most likely plays an important role in the realization of high T_c .^{1,5} However, in Sc_6MTe_2 with $\text{M} = 4d$ and $5d$ transition metals, Sc 3d electrons dominate the electronic state at E_F , and they share a lower T_c of approximately 2 K. In contrast, in the Zr series, both Zr_6RuTe_2 and Zr_6RuBi_2 exhibit the highest T_c in the Zr_6MTe_2 and Zr_6MBi_2 compounds, respectively. The first principles calculations of Zr_6RuBi_2 show that the contribution of the Ru 4d electrons at E_F is comparable to that of the Fe 3d electrons in Sc_6FeTe_2 .¹⁶ The large contribution of the Ru 4d electrons at E_F in Zr_6RuX_2 , which is in contrast to Sc_6RuTe_2 , suggests that the Ru 4d electrons may play an important role in achieving the high T_c values. We hope that further experimental and theoretical studies will elucidate the role of Ru 4d electrons in the superconductivity of Zr_6RuX_2 , which will lead to the discovery of even higher T_c and unconventional superconductors in the A_6MX_2 family.

Acknowledgments

The authors are grateful to Y. Yamakawa, R. Ishii, and Z. Hiroi for helpful discussions. This study was supported by the JSPS KAKENHI (Grant Nos. 23H01831 and 23K26524) and JST ASPIRE (Grant No. JPMJAP2314). The powder XRD experiments were conducted at SPring-8 (Proposal No. 2024B2007) in Hyogo, Japan.

References

- 1) Y. Shinoda, Y. Okamoto, Y. Yamakawa, H. Matsumoto, D. Hirai, and K. Takenaka, J. Phys. Soc. Jpn. **92**, 103701 (2023).

- 2) H. Matsumoto, Y. Yamakawa, R. Okuma, D. Nishio-Hamane, and Y. Okamoto, *J. Phys. Soc. Jpn.* **93**, 023705 (2024).
 - 3) R. Matsumoto, E. Murakami, R. Oishi, S. Ramakrishnan, A. Ikeda, S. Yonezawa, T. Takabatake, T. Onimaru, and M. Nohara, *J. Phys. Soc. Jpn.* **93**, 065001 (2024).
 - 4) K. Yuchi, D. Nishio-Hamane, K. Kojima, K. Moriyama, R. Okuma, and Y. Okamoto, *J. Phys. Soc. Jpn.* **94**, 013701(1-5) (2025).
 - 5) M.-C. Jiang, R. Masuki, G.-Y. Guo, and R. Arita, *Phys. Rev. B* **110**, 104505 (2024).
 - 6) K. Doi, H. Takei, Y. Shinoda, Y. Okamoto, D. Hirai, K. Takenaka, T. Matsushita, Y. Kobayashi, and Y. Shimizu, *Phys. Rev. B* **111**, 214502 (2025).
 - 7) J. N. Graham, K. Yuchi, V. Sazgari, A. Doll, C. Mielke III, P. Král, O. Gerguri, S. S. Islam, V. Pomjakushin, M. L. Medarde, H. Luetkens, Y. Okamoto, and Z. Guguchia, *Adv. Funct. Mater.*, in press.
 - 8) C. Wang and T. Hughbanks, *Inorg. Chem.* **35**, 6987 (1996).
 - 9) V. Petříček, M. Dušek, and L. Palatinus, *Z. Kristallogr. Cryst. Mater.* **229**, 345 (2014).
 - 10) The ZrRu and Zr regions are not discernible in the SEM image.
 - 11) G. Eguchi, D. C. Peets, M. Kriener, Y. Maeno, E. Nishibori, Y. Kumazawa, K. Banno, S. Maki, and H. Sawa, *Phys. Rev. B* **83**, 024512 (2011).
 - 12) Y. Qi, J. Guo, H. Lei, Z. Xiao, T. Kamiya, and H. Hosono, *Phys. Rev. B* **89**, 024517 (2014).
 - 13) Y. Okamoto, T. Inohara, Y. Yamakawa, A. Yamakage, and K. Takenaka, *J. Phys. Soc. Jpn.* **85**, 013704 (2016).
 - 14) N. B. Brandt and N. I. Ginzburg, *Sov. Phys. Usp.* **8**, 202 (1965).
 - 15) Y. Akahama, M. Kobayashi, and H. Kawamura, *J. Phys. Soc. Jpn.* **59**, 3843 (1990).
 - 16) Y. Yamakawa, private communication.
- *email: yuchi@issp.u-tokyo.ac.jp